

Aminated chitosan-g-poly(butyl acrylate) copolymer for heavy oil spills removal: kinetic, isotherm, and thermodynamic investigations

T.M. Tamer^a, A.M. Omer^a, R.E. Khalifa^a, A.A. Ali^b, Y.A. Ammar^c, M.S. Mohy Eldin^{a,*}

^aPolymer Materials Research Department, Advanced Technologies and New Materials Research Institute (ATNMRI), City of Scientific Research and Technological Applications (SRTA-City), New Borg El-Arab City, P.O. Box: 21934, Alexandria, Egypt, emails: mmohyeldin@srtacity.sci.eg (M.S. Mohy Eldin), ttamer85@yahoo.com (T.M. Tamer), ahmedomer_81@yahoo.com (A.M. Omer), randaghonim@gmail.com (R.E. Khalifa)

^bEgyptian General Petroleum Corporation (EGPC), Egypt, email: ahmedabwahed@yahoo.com

^cChemistry Department, Faculty of Science, Al-Azhar University, Egypt, email: yossry@yahoo.com

Received 4 December 2020; Accepted 28 March 2021

ABSTRACT

The kinetic, isotherm, and thermodynamic investigations of the heavy oil spills removal by aminated chitosan-g-poly(butyl acrylate) copolymer have been carried in this study. The kinetic studies of the heavy oil spills removal by both adsorption and absorption processes were carried out using different models namely; pseudo-first-order, pseudo-second-order, and Elovich models. The oil diffusion control process studied by both intraparticle diffusion and Boyd diffusion models. The isotherm of the removal process under equilibrium conditions was investigated by Langmuir, Freundlich isotherm, and Temkin models. Furthermore, the thermodynamic of the process has been also depicted. The obtained results indicated the removal process followed the pseudo-first-order and pseudo-second-order in a very good way and followed both the Langmuir and Freundlich isotherm. The maximum monolayer sorption capacity was found as 41.49, 84.0, and 100.0 g/g for aminated chitosan, aminated chitosan-g-poly(butyl acrylate) 10, and aminated chitosan-g-poly(butyl acrylate) 20, respectively. The thermodynamic studies revealed that sorption was spontaneous and endothermic in nature.

Keywords: Aminated chitosan; Grafting; Kinetics; Isotherm; Thermodynamics

1. Introduction

Water contamination with oil spills is a common and universal problem facing environmental scientists around the world [1]. The toxic impacts of some components of the oil spills or their derivatives on both aquatic lives and on human life, directly or indirectly, are well recognized [2,3]. Such challenge-driven much attention for developing treatment techniques for the oil spills contaminated water ranged from biological to mechanical ones [4–7]. Different materials have been developed and

used as sorbents for oil spills [8,9]. For many reasons and advantages, nature-based sorbents are recommended [10]. Drawbacks such as low hydrophobic character and limited oil sorption capacity compromised the wide application [11]. Many ideas have been investigated to overcome such drawbacks such as induced lauric acid to the structure [12], grafting with acrylate polymers [13–15], and formation of Schiff bases [16]. Among natural-based materials, chitosan comes in the lead for treatment of contaminated waters due to its reach structure with both hydroxyl and amine groups [17–21]. To widen its applicability, many

* Corresponding author.

modifications routes have been investigated including the grafting technique [22–25].

Our previous research project is to develop chitosan derivatives for oil spills applications carried out in two steps. As first step, chitosan modified to have aminated chitosan and nonanyl-chitosan Schiff base [16]. The second step was the grafting of chitosan [20], aminated chitosan [26], and nonanyl-chitosan [27] with hydrophobic–oleophilic polymers poly(butyl acrylate). Furthermore and for a better understanding of the oil spills removal process, the kinetic, isotherm, and thermodynamic parameters have studied for the developed chitosan derivatives [28], chitosan grafted poly(butyl acrylate) [29], and nonanyl-chitosan grafted poly(butyl acrylate) [27].

In the current work, a novel approach has been developed to overcome drawbacks such as low hydrophobic character and limited oil sorption capacity [11]. First, the low hydrophobic character of the chitosan increased through the attachment of the benzene ring of the para-benzoquinone during the amination step, and through the grafting step of poly(butyl acrylate). Furthermore, the limited oil sorption capacity overcome by the acquired oleophilicity of the poly(butyl acrylate) branches grafted to the developed aminated chitosan-g-poly(butyl acrylate) copolymer. Accordingly, the developed adsorbent has two mechanisms of oils spills removal; adsorption through the hydrophobic moieties and absorption through the oleophilic moieties.

For a better understanding of the removal process, the current research aimed to study the kinetic, isotherm, and thermodynamic of the heavy oil spills removal by aminated chitosan-g-poly(butyl acrylate) copolymer to complete our previous studies.

2. Materials and methods

2.1. Materials

Shrimp shells were collected from Marine Waste Sources in Alexandria (Egypt), N-butyl acrylate (98%), p-benzoquinone (PBQ; 99%), potassium persulphate (KPS; 99%) were purchased from Sigma-Aldrich (Germany). Ethylenediamine (EDA; 99%) was purchased from Alfa Aesar (Germany). Sodium hydroxide (99%), ethanol (99%), hydrochloric acid (purity 37%), and acetic acid (98%) were brought from El-Nasr Company (Alexandria). Heavy crude oil was kindly provided by Belayem Petroleum Company (Egypt), with viscosity kinetic at 40°C (Centistokes) equal to 110.

2.2. Methods

2.2.1. Preparation of aminated chitosan (Am-Ch)

First, chitin was extracted from the shell and further deacetylated to have chitosan according to the reported published method [30]. Aminated chitosan derivative obtained based on our previously published method [31].

2.2.2. Preparation of aminated chitosan-poly(butyl acrylate) graft copolymer (Am-Ch-g-BuA)

Two aminated chitosan-poly(butyl acrylate) graft copolymers (Am-Ch-g-BuA) were prepared and encoded as

Am-Ch-g-BuA10 and Am-Ch-g-BuA20 (Table 1). The details of the grafting process were mentioned elsewhere [26].

2.2.3. Batch oil adsorption experiments

The oil adsorption process was achieved based on the Standard Test Method for adsorbent performance (ASTM F726-99) [32] using an oil-artificial seawater system. Various amounts of oil were poured into a 500 mL beaker containing 300 mL of artificial seawater, and then a fixed adsorbent dose was added and spread on the oil–water surface under selected shaking rates at different temperatures ranged from 25°C to 40°C for a known contact time (10–300 min). The heavy crude oil was used to perform the study. The sorption capacity was calculated according to the Standard Method (ASTM F726-99) as follows:

$$\text{Oil sorption capacity (g/g)} = \frac{(W_s - W_w - W_0)}{W_0} \quad (1)$$

where W_s , W_w , and W_0 are the weight of the saturated adsorbent (water + oil + adsorbent), the weight of the adsorbed water, and the initial dry weight of the adsorbent in g, respectively. The quantity of adsorbed water was determined through the extraction separation using n-hexane as the solvent.

3. Results and discussion

3.1. Effect of the sorption time and sorption kinetics

Fig. 1 shows the effect of varying the sorption time on the sorption capacity of the aminated chitosan and its grafted derivatives sorbents. The illustrated data indicate that the grafting process has a positive impact on the sorption capacity which almost duplicated. For all the sorbents, the sorption capacity have been increased with progress of sorption time and reach its maximum values after 3 h. Slight decline of the sorbent capacity was noticed with prolongation of the sorption time to 4 h. It is worthy to mention here that only 30 min are enough for the poly(butyl acrylate) grafted aminated chitosan to remove the same amount of oil performed by chitosan sorbent after 180 min. This is an indication of the fast initial rate of oil sorption of the poly(butyl acrylate) grafted aminated chitosan derivatives. For better understanding of the sorption process, the obtained data were treated by various kinetic models namely; pseudo-first-order, pseudo-second-order, and simple Elovich, models [33,34]; Figs. 2a–c. The kinetic models represented by the following linear form Eqs. (2)–(4);

Table 1
DD and GP (%) of Am-Ch and its grafted copolymers (Am-Ch-g-BuA)

Sample	DD (%)	GP (%)
Am-Ch	91	0.0
Am-Ch-g-BuA10	91	77.0
Am-Ch-g-BuA20	91	93.5

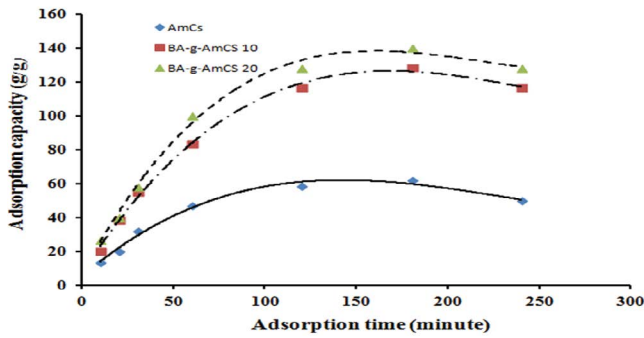


Fig. 1. Effect of the sorption time on the crude oil sorption capacity.

$$\ln(q_e - q_t) = \ln q_e - k_1 t \quad (2)$$

$$\frac{t}{q_t} = \frac{1}{k_2 q_e^2} + \frac{t}{q_e} \quad (3)$$

$$q_t = \beta \ln(\alpha \beta) + \beta \ln t \quad (4)$$

where q_e and q_t (g/g) are the crude heavy oil sorption capacity at equilibrium and time t (min). k_1 (min^{-1}) and k_2 (g/g min) are the constant rate parameters of the pseudo-first-order and the pseudo-second-order sorption. β (g/g) and α (g/g min) are reporting the number of possible adsorptive sites and the sorption extent. The kinetic parameters extracted from the presented Figs. 2a–c were tabulated in Table 2.

From the tabulated results it is obvious that the sorption process data fitted very well with both the pseudo-first-order and the pseudo-second-order models since they provided fit values of the correlation coefficient (all values of R^2 are close to 1). The theoretical (q_{exp}) and the figured (q_{cal}) values of the oil sorption capacity are presented in Table 2 and indicated that the sorption behavior of the Am-Ch sorbent best described by the pseudo-first-order, while the sorption behavior of the poly(butyl acrylate) grafted aminated chitosan derivatives (Am-Ch-g-BuA)

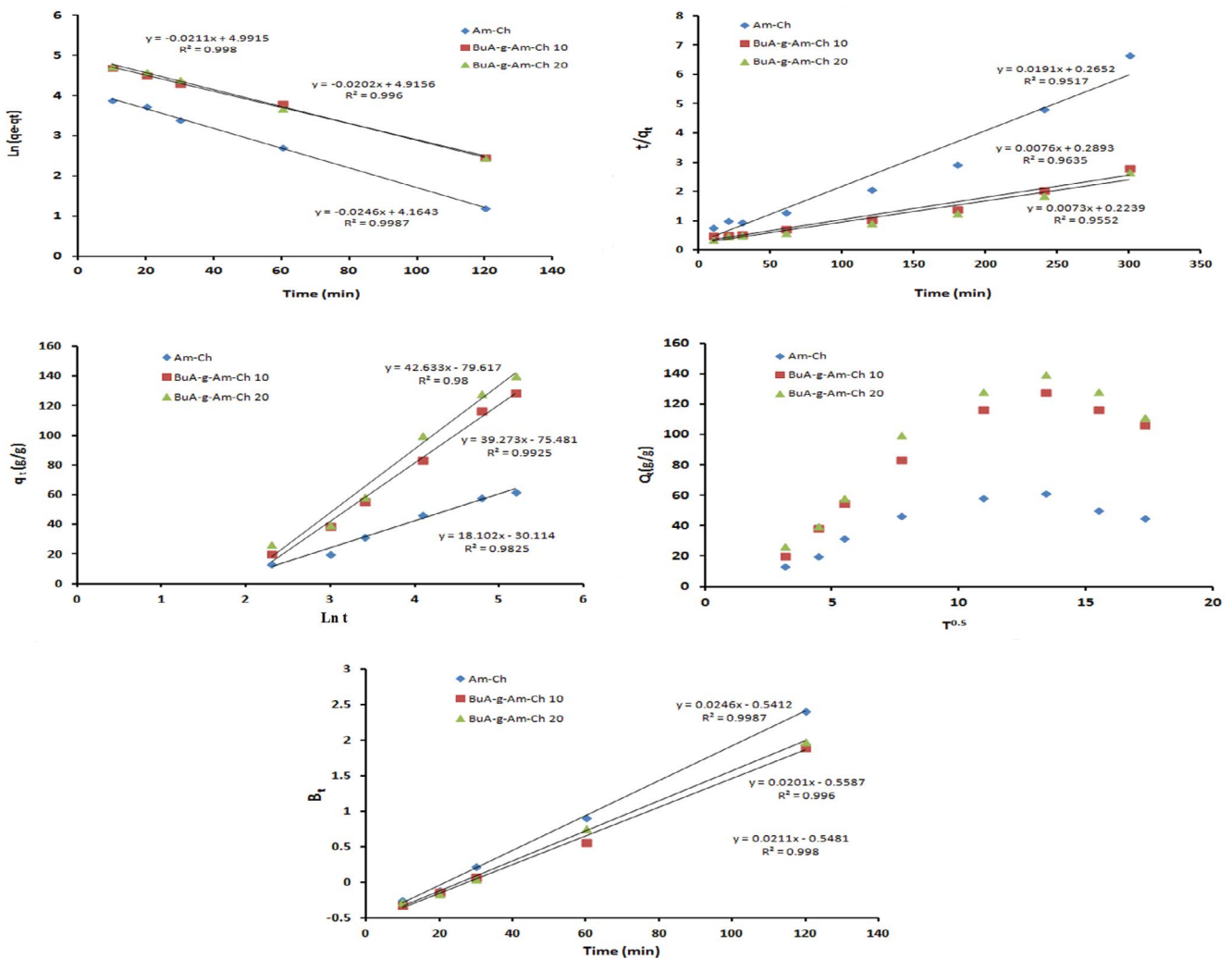


Fig. 2. Kinetics models for the sorption of the crude oil onto the prepared chitosan derivatives; (a) pseudo-first-order, (b) pseudo-second-order model, (c) simple Elovich, (d) intraparticle diffusion model, and (e) Boyd model.

Table 2
Sorption parameters of kinetic models

Kinetic model		Am-Ch	Am-Ch-g-BuA10	Am-Ch-g-BuA20
Isotherm	Parameter	Value		
Pseudo-first-order	$q_{e,cal}$ (g/g)	64.35	136.40	147.16
	$q_{e,exp}$ (g/g)	61.64	128.28	140.00
	k_1 (min ⁻¹)	0.0246	0.0202	0.0211
	R^2	0.9987	0.9960	0.9980
Pseudo-second-order	$q_{e,cal}$ (g/g)	52.36	131.58	137.00
	$q_{e,exp}$ (g/g)	61.64	128.28	140.00
	k_2 (g/g min)	0.2652	0.2893	0.2239
	R^2	0.9552	0.9635	0.9517
Elovich model	α (g/g min)	30.114	75.481	79.617
	β (g/g)	18.102	39.273	42.633
	R^2	0.9825	0.9925	0.9800
Intraparticle diffusion	C	118.36	202.69	238.09
	K_d	4.29	5.55	7.23
	R^2	0.9644	0.9999	0.9814

is best described by the pseudo-second-order models [35,36]. That extracted data indicate the physisorption mechanism of the sorption process by the Am-Ch sorbent turned to be a chemisorption mechanism by the Am-Ch-g-BuA derivatives [37]. The change of the chemical structure and the morphological nature resulted from the grafting process contributed mainly in driven of the sorption process nature from the physisorption mechanism showed by Am-Ch sorbent to the chemisorption mechanism by the Am-Ch-g-BuA derivatives.

The probability that the oil sorption was taking place in the water/oil/Am-Ch sorbents system, and comprising the contribution of other forces, besides the regular Van der Waal's forces, has been assessed by concerning the Elovich model. It assumes that the actual adsorbent surfaces are energetically-heterogeneous. The Elovich equalization does not submit any particular mechanism for the adsorbate-adsorbent reactions. It has comprehensively been established that the chemisorption can be described by this model. The kinetic data plotted in Fig. 2c and the parameters scheduled in Table 2 indicate a good correlation among the theoretical lines and the experimental points. In addition, the correlation coefficient, R^2 values for Am-Ch, Am-Ch-g-BuA10, and Am-Ch-g-BuA20 were agreed with the R^2 values obtained from the pseudo-second-order model. It supposes that the Elovich model well describes the kinetics of the crude oil sorption on the surface of the Am-Ch sorbents [36].

Prediction of the oil diffusion mechanism during the sorption process performed through using two kinetic models namely; intraparticle diffusion [Eq. (5)] and the Boyd model [Eq. (6)] described below [12,38]:

$$q_t = K_p t^{0.5} + C \quad (5)$$

$$B_t = -0.498 - \ln(1 - F) \text{ for } F > 0.85 \quad (6)$$

where K_d (g/g min) is the intraparticle diffusion rate constant and C is the intercept. F is the fraction of solute adsorbed at any time ($F = q_t/q_e$).

Fig. 2d shows two stages curves for Am-Ch and its grafted derivatives. The first, sharper stage is the surface sorption. The kinetic parameters of the intraparticle diffusion extracted from the second straight line stage (Table 2). The K_d values (Table 2) are 4.26, 5.55, and 7.23 (g/g min) for Am-Ch, Am-Ch-g-BuA10, and Am-Ch-g-BuA20, successively. The presented data verified that Am-Ch grafted copolymers support enhanced the sorption of the crude oil compared with the Am-Ch based sorbent. This is in agreement with the results published by Itodo et al. [39]. Also, all the linear curves not passed through the origin, that is, ($C > 0$) which proved attributable to the difference in the mass transfer rate from the initial to final sorption stages [39]. Further, the depth of the boundary layer is extracted from the intercept values. Table 2 indicated that the boundary layer thickness tends to be greater in the case of the grafted derivatives sorbents. According to Itodo et al. [39] assumption, the presented data in Table 2 indicate that the transport mode is governed by more than one process which means that two or more steps transpire [40]. Besides, it indicates that the intraparticle diffusion is not the only rate defining step.

To determine which step is the controlling one in the oil diffusion process, the sorption data were fitted by Boyd kinetic model; Fig. 2e. The figure shows that straight lines obtained which did not pass through the origin. That observation confirmed that the film-diffusion is the rate-controlling mechanism. Other authors investigated this issue [41,42].

3.2. Effect of the initial oil concentration and sorption isotherms

Fig. 3 demonstrates the impact of varying the oil concentration on the sorption capacity of the Am-Ch and its grafted derivatives. From the Fig. 3, we can see that the

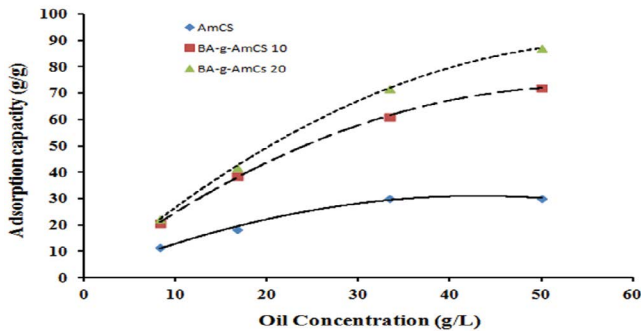


Fig. 3. Effect of the initial crude oil concentration on the sorption equilibrium.

increase of the oil concentration from 8.33 to 33.32 g/L has a positive linear effect on the sorption capacity of the used sorbents. Further increment of the oil concentration, up to 50 g/L, showed a slower increment of the sorption capacity. The figure also demonstrated a clear positive impact of the grafting process where the sorption capacity of the grafted sorbents, Am-Ch-g-BuA10, and Am-Ch-g-BuA20, is 2.4 and 2.9 folds of the Am-Ch based sorbent. This finding strongly supports the benefits of the grafting modification technique. Two main causes for such improvement could be mentioned here; the hydrophobicity of the BuA graft branches [43], in addition to its oleophilic nature [33,38]:

To describe the adsorption process and understand its nature, the relation between the oil spills and the sorbents surface and consequently their sorption capacities, the illustrated data in Fig. 3 fitted with different isotherm models. Three isotherm models, linear form, have been used

according to the following equations: Langmuir [Eq. (7)] Freundlich [Eq. (8)], and Temkin [Eq. (9)] [35,44].

$$\frac{C_e}{q_e} = \frac{1}{q_{\max} K_L} + \frac{C_e}{q_{\max}} \tag{7}$$

$$\ln q_e = \ln K_F + \frac{1}{n} \ln C_e \tag{8}$$

$$q_e = B_T \ln K_T + B_T \ln C_e \tag{9}$$

where q_{\max} (g/g), C_e (g/L), and K_L (L/g) is the saturated sorption capacity, the crude oil concentration at equilibrium, and the Langmuir isotherm constant, respectively. $1/n$ and K_F are the Freundlich constants belonged to sorption intensity and sorption capacity. B (J/mol) is the heat of sorption, and K_T (L/g) is the highest binding energy of adsorbent and adsorbate.

The data illustrated in Figs. 4a–c where the isotherm parameters extracted and tabulated in Table 3. The data show that the Langmuir isotherm described very well of the sorption process. The correlation coefficients (R^2) are close to 1.0 for all the sorbents. That finding indicates the strong attraction between the oil spills and the sorbents surface. Furthermore, confirms the affinity of the sorbents toward the sorption of the oil dispersed in the aqueous medium [45]. On the other hand, the fundamental characteristics of the Langmuir isotherm, the dimensionless separation factor (R_L), can be expressed by Eq. (10) and tabulated in Table 4.

$$R_L = \frac{1}{1 + K_L C_0} \tag{10}$$

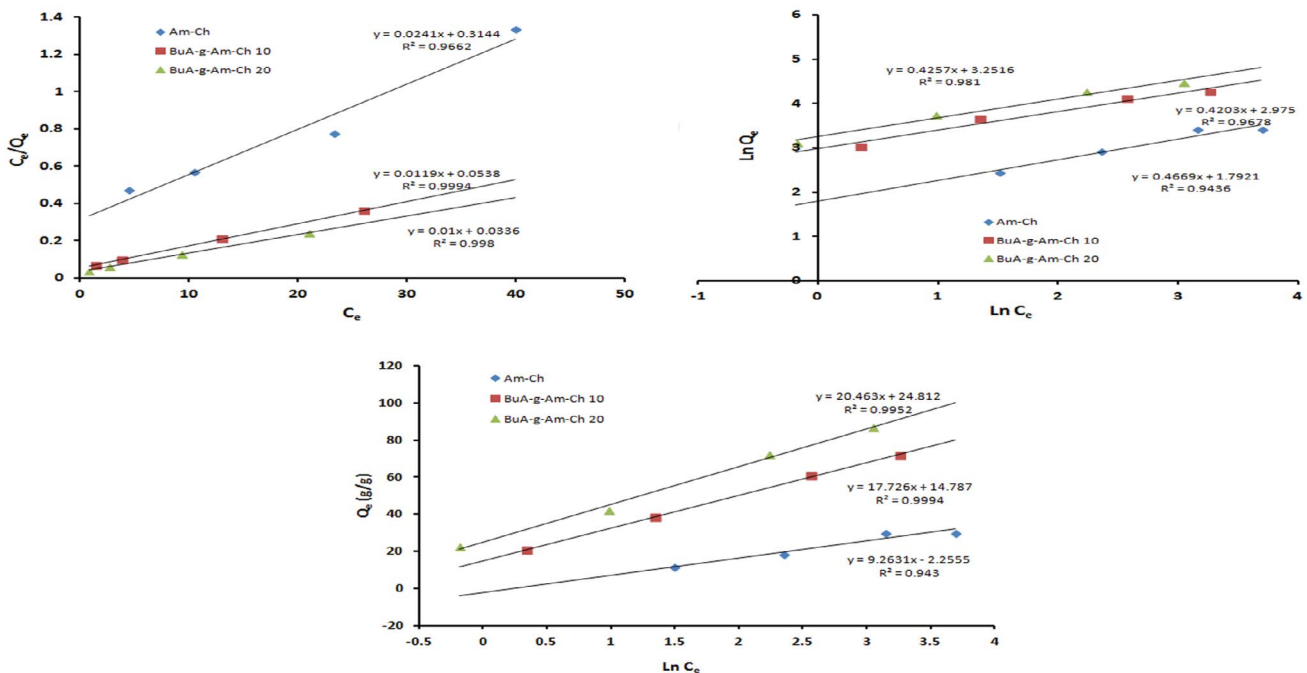


Fig. 4. Equilibrium isotherms for the sorption of the crude oil onto the prepared chitosan derivatives; (a) Langmuir, (b) Freundlich, and (c) Temkin isotherms.

Table 3
Parameters of the different isotherm models and correlation coefficients for the sorption of the crude oil

Adsorbent type		Am-Ch	Am-Ch-g-BuA10	Am-Ch-g-BuA20
Isotherm	Parameter	Value		
Langmuir	q_{\max} (g/g)	41.49	84.03	100
	K_L (L/g)	13.05	4.52	3.36
	R^2	0.998	0.999	0.966
Freundlich	K_F (g/g)	6.00	19.60	25.82
	$1/n$	0.467	0.420	0.426
	R^2	0.9436	0.9678	0.9810
Temkin	K_T (L/g)	0.7839	2.303	3.362
	B_T (J/mol)	9.263	17.726	20.463
	R^2	0.943	0.999	0.995

Table 4 indicates the R_L values were between 0.0 and 1.0 demonstrating the favourable sorption of the crude oil on the used sorbents. The obtained R^2 values of Langmuir isotherm and the Freundlich isotherm model are higher than 0.94 which postulate that both monolayer and multilayer sorption played a very important role in the crude oil-uptake by all the used sorbents [35]. The maximum monolayer sorption capacities were obtained to be 41.5, 84.0, and 100 g/g for Am-Ch, Am-Ch-g-BuA10, and Am-Ch-g-BuA20, respectively. Furthermore, the high adsorbent/adsorbate interaction confirmed by the positive and higher values of the B_T parameter obtained from the Temkin plot (Table 3).

3.3. Effect of the sorption medium temperature and thermodynamics

The behaviour of the oil sorption process for all sorbent samples was evaluated under different sorption medium temperatures ranged from 25°C to 40°C as shown in Fig. 5. The maximum sorption capacity was detected at 35°C. A slight decline noticed with a further acceleration of temperature to 40°C. These consequences could be described by promoting the segmental movement for all analyzed adsorbents, where the diffusion rate of oil spill molecules into the adsorbent surface enhanced with raising the temperature up to 35°C [44].

The thermodynamic parameters (Table 5) investigated from Fig. 6 incline and intercept were determined using the following equations [43]:

$$K_D = \frac{Q_e}{C_e} \quad (11)$$

$$\ln K_D = -\frac{\Delta H}{RT} + \frac{\Delta S}{R} \quad (12)$$

where ΔG and ΔH are in kJ/mol, ΔS is in J/mol K, T is the sorption temperature in K, and R is the universal gas constant (8.314 J/mol).

Information extracted from the negative ΔG values, for used sorbents; imply that we have a spontaneous sorption

Table 4
 R_L values of the Freundlich isotherm

C_0 (g/L)	R_L		
	Am-Ch	Am-Ch-g-BuA10	Am-Ch-g-BuA20
8.33	0.0091	0.0259	0.0345
16.66	0.0046	0.0131	0.0176
33.32	0.0023	0.0066	0.0089
50	0.0015	0.0044	0.0059

process. On the other hand, the endothermic nature of the sorption process reflected by the positive values of the ΔG . That finding explained the positive impact of elevation sorption temperature on the oil sorption capacity [44]. In addition, it is indicated also the complication of the sorption due to simultaneous chemical and physical reactions. Furthermore, the interface between sorbents and oil spills tends to be more random during the oil removal process. However, the positive value of ΔS intends the increase in randomness at the adsorbent/adsorbed interface during the sorption process [46].

3.4. Sorption capacity comparative study

The obtained maximum monolayer sorption capacity in this study by Am-Ch and its graft copolymers derivatives has been compared with other bio-based adsorbents developed by other authors (Table 6). It can be seen that our developed Am-Ch graft copolymers derivatives show high sorption capacity than most compared sorbents [47,48,50,51] and less than others especially the porous one [49]. However, this comparison is unfair owing to the diversity of the operating conditions and the chemical composition of the compared sorbents.

4. Conclusion

Chitosan bio-based graft copolymers sorbents have been developed through grafting aminated chitosan with butyl acrylate. The developed derivatives have been tested

Table 5
Thermodynamic parameters of the sorption capacity for the crude oil by various chitosan adsorbents

T (K)	Thermodynamic parameters								
	Am-Ch			Am-Ch-g-BuA10			Am-Ch-g-BuA20		
	ΔG (kJ/mol)	ΔH (kJ/mol)	ΔS (J/mol K)	ΔG (kJ/mol)	ΔH (kJ/mol)	ΔS (J/mol K)	ΔG (kJ/mol)	ΔH (kJ/mol)	ΔS (J/mol K)
298	-37.951			-98.657			-101.125		
303	-38.588	34.344	127.35	-100.312	91.072	331.06	-102.821	92.917	339.344
308	-39.225			-101.968			-104.518		
313	-39.862			-103.623			-106.215		

Table 6
Comparison of the maximum sorption capacity for the crude oil by various bio-based sorbents

Adsorbent	Sorption capacity	Reference
Chitosan (prawn shells)	18.52 g/g	[47]
Cellulose aerogel functionalized with methyltrimethoxysilane	24.4 g/g	[48]
Biochar	166 mg/g	[49]
BuAc-cellulose graft copolymer	13.83 g/g	[50]
Nanobentonite incorporated nanocellulose chitosan based aerogel	50 g/g	[51] ^a
Aminated chitosan (Am-Ch)	41.49 g/g	This study
Am-Ch-g-BuA10	84.03 g/g	This study
Am-Ch-g-BuA20	100.00 g/g	This study

^aspent engine oil and silicone oil used in this study.

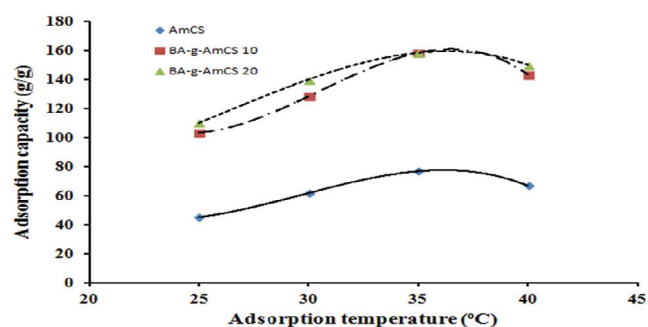


Fig. 5. Effect of the sorption temperature on the crude oil sorption capacity.

in the removal of crude heavy oil spills from saline water. Through the study, the kinetic, isotherm, and thermodynamic characterization of the oil sorption process have been performed. The kinetic studies using pseudo-first-order, pseudo-second-order, and Elovich models show that the sorption process followed basically the pseudo-second-order law. The oil diffusion process studied by both intraparticle diffusion and Boyd diffusion models shows that the film-diffusion is the rate-controlling mechanism. The isotherm of the removal process under equilibrium conditions was followed by both the Langmuir and Freundlich isotherm. The maximum monolayer sorption capacity could be arranged in the following order; aminated chitosan < aminated chitosan-g-poly(butyl acrylate) 10 < aminated

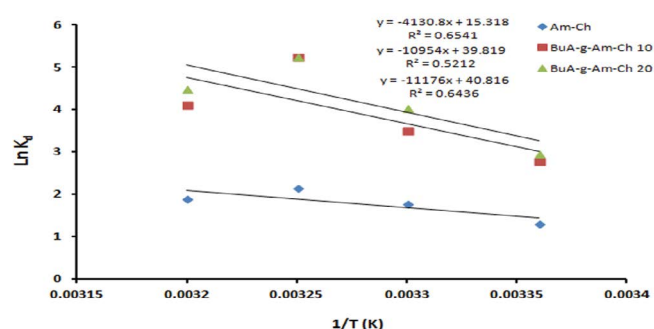


Fig. 6. Thermodynamics of the sorption of the crude oil onto the prepared chitosan derivatives.

chitosan-g-poly(butyl acrylate) 20. Furthermore, the thermodynamic of the process revealed that the sorption process was spontaneous and endothermic in nature.

References

- [1] H.I. Kelle, Mopping of crude oil and some refined petroleum products from the environment using sawmill factory waste: adsorption isotherm and kinetic studies, *J. Appl. Sci. Environ. Manage.*, 22 (2018) 34–40.
- [2] Q. Hao, Y. Song, Z. Mo, S. Mishra, J. Pang, Y. Liu, J. Lian, J. Wu, S. Yuan, H. Xu, H. Li, Highly efficient adsorption of oils and pollutants by porous ultrathin oxygen-modified BCN nanosheets, *ACS Sustainable Chem. Eng.*, 7 (2019) 3234–3242.

- [3] E.T. Nwankwere, C.E. Gimba, G.I. Ndukwe, A.K. Isuwa, Modeling of the kinetic and equilibrium sorption behavior of crude oil on HDTMAB modified Nigerian nanoclays, *Int. J. Sci. Technol. Res.*, 4 (2015) 106–114.
- [4] G. Ju, J. Liu, D. Li, M. Cheng, F. Shi, Chemical and equipment free strategy to fabricate water/oil separating materials for emergent oil spill accidents, *Langmuir*, 33 (2017) 2664–2670.
- [5] O. Carmody, R. Frost, Y. Xi, K. Serge, Adsorption of hydrocarbons on organo-clays-implications for oil spill remediation, *J. Colloid Interface Sci.*, 305 (2007) 17–24.
- [6] B.T. Song, Q. Xu, Highly hydrophobic and superoleophilic nanofibrous mats with controllable pore sizes for efficient oil/water separation, *Langmuir*, 32 (2016) 9960–9966.
- [7] D. Ceylan, S. Dogu, B. Karacik, S.D. Yakan, O.S. Okay, O. Okay, Evaluation of butyl rubber as sorbent material for the removal of oil and polycyclic aromatic hydrocarbons from seawater, *Environ. Sci. Technol.*, 43 (2009) 3846–3852.
- [8] R.K. Gupta, G.J. Dunderdale, M.W. England, A. Hozumi, Oil/water separation techniques: a review of recent progresses and future directions, *J. Mater. Chem. A*, 5 (2017) 16025–16058.
- [9] Q.F. Wei, R.R. Mather, A.F. Fotheringham, R.D. Yang, Evaluation of nonwoven polypropylene oil sorbents in marine oil-spill recovery, *Mar. Pollut. Bull.*, 46 (2003) 780–783.
- [10] B. Doshi, M. Sillanpää, S. Kalliola, A review of bio-based materials for oil spill treatment, *Water Res.*, 135 (2018) 262–277.
- [11] P. Venkataraman, J. Tang, E. Frenkel, G.L. McPherson, J. He, S.R. Raghavan, V. Kolesnichenko, A. Bose, V.T. John, Attachment of a hydrophobically modified biopolymer at the oil-water interface in the treatment of oil spills, *ACS Appl. Mater. Interfaces*, 5 (2013) 3572–3580.
- [12] S.M. Sidik, A.A. Jalil, S. Triwahyono, S.H. Adam, M.A.H. Satar, B.H. Hameed, Modified oil palm leaves adsorbent with enhanced hydrophobicity for crude oil removal, *Chem. Eng. J.*, 203 (2012) 9–18.
- [13] M. Keshawy, T.A. El-Moghny, A.-R.M. Abdul-Raheim, K. Kabel, S.H. El-Hamouly, Synthesis and characterization of oil sorbent based on hydroxypropyl cellulose acrylate, *Egypt. J. Pet.*, 22 (2013) 539–548.
- [14] H.H. Sokker, N.M. El-Sawy, M.A. Hassan, B.E. El-Anadouli, Adsorption of crude oil from aqueous solution by hydrogel of chitosan based polyacrylamide prepared by radiation induced graft polymerization, *J. Hazard. Mater.*, 190 (2011) 359–365.
- [15] G.S. Chauhan, B. Singh, S. Kumar, A. Chinkara, Synthesis and characterization of reactive copolymers of poly(butyl acrylate) and cellulose, *Polym. Polym. Compos.*, 13 (2005) 467–477.
- [16] M.S. Mohy Eldin, Y.A. Ammar, T.M. Tamer, A.M. Omer, A.A. Ali, Development of low-cost chitosan derivatives based on marine waste sources as oil adsorptive materials: I. preparation and characterization, *Desal. Water Treat.*, 72 (2017) 41–51.
- [17] X.X. Liang, A.M. Omer, Z. Hu, Y. Wang, D. Yu, X. Ouyang, Efficient adsorption of diclofenac sodium from aqueous solutions using magnetic amine-functionalized chitosan, *Chemosphere*, 217 (2018) 270–278.
- [18] A. Eskhan, F. Banat, M. Abu Haija, S. Al-Asheh, Synthesis of mesoporous/macroporous microparticles using three dimensional assembly of chitosan-functionalized halloysite nanotubes and their performance in the adsorptive removal of oil droplets from water, *Langmuir*, 35 (2019) 2343–2357.
- [19] V.K. Mourya, N.N. Inamdar, Chitosan-modifications and applications: opportunities galore, *React. Funct. Polym.*, 68 (2008) 1013–1051.
- [20] M.S. Mohy Eldin, Y.A. Ammar, T.M. Tamer, A.M. Omer, A.A. Ali, Development of oleophilic adsorbent based on chitosan-poly(butyl acrylate) graft copolymer for petroleum oil spill removal, *Int. J. Adv. Res.*, 4 (2016) 2095–2111.
- [21] S.W. Benner, V.T. John, C.K. Hall, Simulation study of hydrophobically modified chitosan as an oil dispersant additive, *J. Phys. Chem. B*, 119 (2015) 6979–6990.
- [22] M.T. Tamer, V. Katarina, A.H. Mohamed, M.O. Ahmed, E.-S. Muhammad, S.M.-E. Mohamed, Š. Ladislav, Chitosan/hyaluronan/edaravone membranes for anti-inflammatory wound dressing: in vitro and in vivo evaluation studies, *Mater. Sci. Eng., C*, 90 (2018) 227–235.
- [23] D.W. Jenkins, M.H. Samuel, Review of vinyl graft copolymerization featuring recent advances toward controlled radical-based reactions and illustrated with chitin/chitosan, *Trunk Polymers Chem. Rev.*, 101 (2001) 3245–3273.
- [24] R. Nithya, P.N. Sudha, Grafting of N-butyl acrylate on to chitosan by ceric Ion initiation and its antimicrobial activity, *Der Pharm. Lett.*, 6 (2014) 58–64.
- [25] A.H. Mohamed, M.O. Ahmed, A. Eman, M.A.B. Walid, M.T. Tamer, Preparation, physicochemical characterization and antimicrobial activities of novel two phenolic chitosan Schiff base derivatives, *Sci. Rep.*, 8 (2018) 1–14.
- [26] M.S. Mohy Eldin, Y.A. Ammar, T.M. Tamer, A.M. Omer, A.A. Ali, Development of low-cost oleophilic adsorbent based on aminated chitosan-poly(butyl acrylate) graft copolymer for marine oil spill clean-up, *Int. J. Adv. Res.*, 4 (2016) 2080–2094.
- [27] A.M. Omer, R.E. Khalifa, T.M. Tamer, M. Elnouby, A.M. Hamed, Y.A. Ammar, A.A. Ali, M. Gouda, M.S. Mohy Eldin, Fabrication of a novel low-cost superoleophilic nonanyl chitosan poly(butyl acrylate) grafted copolymer for the adsorptive removal of crude oil spills, *Int. J. Biol. Macromol.*, 140 (2019) 588–599.
- [28] R.E. Khalifa, A.M. Omer, T.M. Tamer, A.A. Ali, Y.A. Ammar, M.S. Mohy Eldin, Efficient eco-friendly crude oil adsorptive chitosan derivatives: kinetics, equilibrium and thermodynamic studies, *Desal. Water Treat.*, 159 (2019) 269–281.
- [29] A.M. Omer, R.E. Khalifa, T.M. Tamer, A.A. Ali, Y.A. Ammar, M.S. Mohy Eldin, Kinetic and thermodynamic studies for the sorptive removal of crude oil spills using a low-cost chitosan-poly(butyl acrylate) grafted copolymer, *Desal. Water Treat.*, 192 (2020) 213–225.
- [30] M.M. Islam, S.M. Masum, M.M. Rahman, M.A.I. Molla, A.A. Shaikh, S.K. Roy, Preparation of chitosan from shrimp shell and investigation of its properties, *Int. J. Basic Appl. Sci.*, 11 (2011) 77–80.
- [31] M.S. Mohy Eldin, E.A. Soliman, A.I. Hashem, T.M. Tamer, Antimicrobial activity of novel aminated chitosan derivatives for biomedical applications, *Adv. Polym. Technol.*, 31 (2012) 414–428.
- [32] B. Alireza, T. Jun, M. Gordon, Standardization of oil sorbent performance testing, *J. Test. Eval.*, 43 (2015) 1–8.
- [33] N.E. Thompson, G.C. Emmanuel, K.J. Adagadzu, N.B. Yusuf, Sorption studies of crude oil on acetylated rice husks, *Arch. Appl. Sci. Res.*, 2 (2010) 142–151.
- [34] H. Li, X. Zhuang, M. Bao, Kinetics and thermodynamics of dissolved petroleum hydrocarbons in sediment under sophorolipid application and their effects on oil behavior end results in marine environment, *RSC Adv.*, 7 (2017) 45843–45851.
- [35] R.E. Khalifa, A.M. Omer, T.M. Tamer, W.M. Salem, M.S. Mohy Eldin, Removal of methylene blue dye from synthetic aqueous solutions using novel phosphonate cellulose acetate membranes: adsorption kinetic, equilibrium, and thermodynamic studies, *Desal. Water Treat.*, 144 (2019) 272–285.
- [36] S.M. Davoodi, M. Taheran, S.K. Brar, R. Galvez-Cloutier, R. Martel, Hydrophobic dolomite sorbent for oil spill clean-ups: kinetic modeling and isotherm study, *Fuel*, 251 (2019) 57–72.
- [37] S.C. Cheu, H. Kong, S.T. Song, K. Johari, N. Saman, M.A.C. Yunus, Separation of dissolved oil from aqueous solution by sorption onto acetylated lignocellulosic biomass: equilibrium, kinetics and mechanism studies, *J. Environ. Chem. Eng.*, 4 (2016) 868–881.
- [38] Ş. Taşar, F. Kaya, A. Özer, Biosorption of lead(II) ions from aqueous solution by peanut shells: equilibrium, thermodynamic and kinetic studies, *J. Environ. Chem. Eng.*, 2 (2014) 1018–1026.
- [39] A.U. Itodo, F.W. Abdulrahman, L.G. Hassan, S.A. Maigandi, H.U. Itodo, Intraparticle diffusion and intraparticle diffusivities of herbicide on derived activated carbon, *Research*, 2 (2010) 74–86.
- [40] D.C. Sinica, C. Imaga, A.A. Abia, J.C. Igwe, Removal of Ni(II), Cu(II) and Zn(II) ions from synthetic wastewater using sorghum hulls as adsorbents, *Der Chem. Sin.*, 5 (2014) 67–75.
- [41] M.A. Ahmad, P.N.A. Ahmad, O.S. Bello, Kinetic, equilibrium and thermodynamic studies of synthetic dye removal using

- pomegranate peel activated carbon prepared by microwave induced KOH activation, *Water Resour. Ind.*, 6 (2014) 18–35.
- [42] S. Karthikeyan, B. Sivakumar, N. Sivakumar, Film and pore diffusion modeling for adsorption of reactive red 2 from aqueous solution on to activated carbon prepared from biodiesel industrial waste, *J. Chem.*, 7 (2012) S175–S184.
- [43] A. Ummadisingu, S. Gupta, Characteristics and kinetic study of chitosan prepared from seafood industry waste for oil spills cleanup, *Desal. Water Treat.*, 44 (2012) 44–51.
- [44] A. Achmad, J. Kassim, T.K. Suan, R.C. Amat, T.L. See, Equilibrium, kinetic and thermodynamic studies on the adsorption of direct dye onto a novel green adsorbent developed from *Uncaria gambir* extract, *J. Phys. Sci.*, 23 (2012) 1–13.
- [45] S.S. Elanchezhian, N. Sivasurian, S. Meenakshi, Enhancement of oil recovery using zirconium-chitosan hybrid composite by adsorptive method, *Carbohydr. Polym.*, 145 (2016) 103–113.
- [46] N. Lv, X. Wang, S. Peng, H. Zhang, L. Luo, Study of the kinetics and equilibrium of the adsorption of oils onto hydrophobic jute fiber modified via the sol-gel method, *Int. J. Environ. Res. Public Health*, 15 (2018) 969–983.
- [47] V.K. Gupta, A. Mittal, A. Malviya, J. Mittal, Adsorption of carmoisine A from wastewater using waste materials-bottom ash and deoiled soya, *J. Colloid Interface Sci.*, 335 (2009) 24–33.
- [48] T.N. Son, F. Jingduo, T.L. Nhat, T.T.L. Ai, H. Nguyen, B.C.T. Vincent, M.D. Hai, Cellulose aerogel from paper waste for crude oil spill cleaning, *Ind. Eng. Chem. Res.*, 52 (2013) 18386–18391.
- [49] L. Silvani, B. Vrchotova, P. Kastanek, K. Demnerova, I. Pettiti, M.P. Papini, Characterizing biochar as alternative sorbent for oil spill remediation, *Sci. Rep.*, 7 (2017) 1–10.
- [50] G. Yuan, Z. Yitong, Z. Xiaoli, Z. Liping, Q. Ping, Synthesis and characteristics of graft copolymers of poly(butyl acrylate) and cellulose fiber with ultrasonic processing as a material for oil absorption, *Bioresources*, 7 (2012) 135–147.
- [51] V. Sharma, T. Shahnaz, S. Subbiah, S. Narayanasamy, New insights into the remediation of water pollutants using nanobentonite incorporated nanocellulose chitosan based aerogel, *J. Polym. Environ.*, 28 (2020) 2008–2019.